Teleconnections and the Arctic Oscillation Analyzed in the Barotropic Component of the Model and Observed Atmosphere

H. L. Tanaka[1] **and Ippo Suzuki**[2]

1: Center for Computational Sciences,

University of Tsukuba, Japan

2: Graduate School of Environmental Sciences

University of Tsukuba, Japan

Submitted: 27 May 2007

AOFD 2007 Proceeding

Abstract

In this study, teleconnectivity and one point correlations are analyzed for the barotropic component of the atmosphere represented by a simple barotropic model (called barotropic S-model), and the results are compared with observation by the NCEP/NCAR reanalysis. It is confirmed that the teleconnectivity and the PNA pattern are simulated reasonably by the barotropic S-model. The question is focused whether the Arctic Oscillation (AO) would appear by the one point correlation in the model atmosphere. According to the result, it is found that the one point correlation is not restricted within the Atlantic sector like the NAO, but spread to entire mid-latitudes surrounding the Arctic. The positive correlations in the Pacific sector are all statistically significant at the 5% confidence level. The result suggests that the AO represented by the barotropic S-model is not a statistical artifact due to the multiple teleconnections of the NAO and PNA, but a physical mode with dynamical basis. The reason for the reduced correlation in the observation is inferred in discussion.

1. Introduction

Atmospheric teleconnections are prominent recurrent patterns in the general circulation, which is measured by one point correlation with surrounding remote areas. North Atlantic Oscillation (NAO) and the Pacific/North American (PNA) patterns are the most notable teleconnections appearing in the sea level pressure and 500 hPa height, respectively. The problem is whether the Arctic Oscillation (AO by Thompson and Wallace 1998) is a physical mode with true dynamical basis or a statistical artifact by a combination of multiple teleconnections of the NAO and PNA.

According to Deser (2000), the NAO is clearly qualified as a teleconnection showing the correlation of -0.83 between the Arctic and Atlantic sectors for the winter-mean data. Yet, the AO is not qualified as a teleconnection because the correlation between the Atlantic and Pacific sectors is only -0.07, where the statistical significance at the 5% confidence level is 0.22 and more. Itoh (2002) clearly explained the statistical trick of the AO using a three-point correlation model followed by a detailed analysis of teleconnectivity between the Atlantic and Pacific sectors by removing the data in the Arctic region. They concluded that the AO is not a dynamical mode but a statistical artifact by the multiple teleconnections.

Against this controversial problem, a dynamical explanation was pursued by Kimoto et al. (2001) and Watanabe and Jin (2004), proposing a neutral mode theory based on the SVD (singular value decomposition) analysis. Tanaka and Matsueda (2005) solved singular modes and eigenmodes of the linearized dynamical system, which is now referred to as a singular eigenmode theory. The essential features of the AO are contained in the barotropic component of the atmosphere governed by the 2D fluid mechanics which characterizes the low-frequency variability. Using a simple barotropic model derived from the 3D normal mode expansion, Tanaka (2003) conducted a numerical simulation of the AO and obtained the same structure as observed in the atmosphere (see Figs. 1 and 2). Tanaka and Matsueda (2005) identified that the characteristics of the AO are originated from the eigenmode of the dynamical system with nearly zero eigenvalue , i.e., singular eigenmode, for the global atmosphere.

Hence, the problem is whether the insignificant correlation between the Atlantic and Pacific sectors by Deser (2000) is true or not for the barotropic component of the model and observed atmosphere. The purpose of this study is to examine the teleconnectivity and the one point correlations in the observed atmosphere and in the model atmosphere reproduced by the barotropic S-model in order to understand the AO.

2. Model and data

The model used in this study is identical to that in Tanaka (2003). It is a 3D representation of the spectral primitive equations on a sphere, which may be written as:

$$\frac{dw_i}{d\tau} = -i\sigma_i w_i - i\sum_{jk} r_{ijk} w_j w_k + f_i, \tag{1}$$

where w_i is the complex state variable of the system obtained as the Fourier expansion coefficients of meteorological variables, σ_i is the eigenfrequency of the Laplace's tidal equation, f_i is the expansion coefficient of the external forcing of viscosity and diabatic heating rate, and r_{ijk} is the interaction coefficients for the nonlinear terms. There should be no confusion in the use of i for the subscript even though it is used for the imaginary unit in (1). The equation is then closed using only the barotropic component of w_i.

Four-time daily NCEP/NCAR reanalysis for 51 years from 1950 to 2000 (Kalnay et al. 1996) are used to compute w_i.

The external forcing f_i is evaluated as the residual balance of (1). Then, the time series of f_i is regressed by w_i so that the regression error is minimized. The model so constructed is called a barotropic S-model because the external forcing is evaluated statistically from the long-term observational data.

Once the model is constructed, the nonlinear system (1) is integrated for 50 years from the initial condition of 1 January 1950 under the perpetual January condition.

3. Comparison of the EOF patterns

The EOF-1 of the daily time series of w_i for the observed and model atmosphere are presented in Fig. 1a and b, respectively. Note that the analysis period is slightly longer in this study compared to Tanaka (2003). The same period corresponding to DJF is used for the analysis, although it is a perpetual January run.

As demonstrated by Tanaka (2003), the barotropic S-model reproduces the AO pattern, despite its quite simple formulation. The EOF-1 is identified as the AO, and the structure is almost identical with the singular eigenmode solution by Tanaka and Matsueda (2005). The positive anomaly over the Azores High extends westward, and a separated positive center is seen in the model atmosphere. Likewise, the positive anomaly over the Pacific is elongated westward in the model atmosphere. These minor differences are reasonable because the structure of the observed AO is also deformed as seen in the model atmosphere for different analysis period during winter such as monthly data instead of DJF. The variances explained by the EOF-1 are 5.7% and 15.1% for the observation and model, respectively, when the daily data are analyzed. The contribution increases from

5.7% to 21% when the seasonal (DJF) mean data are analyzed for the observation (see Tanaka 2003).

The EOF-2 of the daily time series of the observed and model atmosphere are presented in Fig. 2a and b, respectively. The EOF-2 is characterized by the negative correlation between the Pacific and Atlantic sectors. The PNA pattern is embedded in part of the EOF-2 from North Pacific to the southwestern Atlantic. Another wavetrain is seen from North Atlantic via the Arctic to Siberia. The variances explained by the EOF-2 are 4.3% and 8.4% for the observation and model, respectively. The larger variance in the model is explained by the same reason as in EOF-1, with active transient short waves in observation, which is damped in the model.

It may be shown that the model can reproduce not only the EOF-1 and EOF-2, but also up to EOF-4 of the observed low-frequency variability. The result supports the further analysis of the low-frequency variability and the teleconnections in the model atmosphere to compare with observation.

4. Teleconnectivity

Next, we compare the atmospheric teleconnectivity for the model and the observed atmosphere using monthly-mean data during the winter (DJF) from 1950 to 2000. According to Wallace and Gutzler (1981), the teleconnectivity T_i is defined as:

$$T_i = \mid (R_{ij}) \ \ min \text{ for all } j \mid, \tag{2}$$

where R_{ij} are the correlation coefficients at any selected grid point (denoted by the subscript i) and those at every other grid points in the hemisphere (denoted by the subscript j). The results of the teleconnectivity are illustrated in percentile for the model and observed atmosphere (not shown). There are 2 maxima of the teleconnectivity in the Pacific sector corresponding to the PNA, and other 2 in the Atlantic sector corresponding to the NAO. The values of the model are slightly larger than the observation due to the less transient short-wave noise in the model as mentioned in Section 3. Although some differences may be noted, the overall patterns are almost identical for the model and observed atmosphere. The model atmosphere appears to represent the low-frequency variability and teleconnections in pure shape without the high-frequency transient noise.

5. One point correlations

In this Section, one point correlations are examined for the PNA and NAO or AO. The locations of the center points are listed in Table 1 for the model and observation in reference to the results in the teleconnectivity. Figure 3 illustrates the one point correlation maps for the PNA. The target grid points are chosen from the North Pacific peaks of the teleconnectivity. Monthly mean data for DJF during 50 years are used for the correlation with 150 degree of freedom. The result shows clear wavetrain from the North Pacific via Canada to the southwestern Atlantic. The agreement for the PNA patterns is almost perfect for the model and observation. The model shows slightly higher correlations at Canada and southwestern Atlantic since the low-frequency variability is simulated in pure form with less transient noise. We note that there is a positive correlation in Europe which is statistically significant.

Figure 4 illustrates the one point correlation maps for the NAO or AO. The target grid points are chosen from the positive center of action of the barotropic height in Fig. 1a and 1b at the eastern Atlantic. It is important to note from the result that the correlation pattern in Fig. 4b for the model is quite similar to the AO pattern in Fig. 1, showing a negative pole over Greenland representing NAO and three positive poles at the Far East, western Pacific and southern USA. The result suggests that the EOF-1 of the AO mode is a physical mode at least for the model atmosphere. When the correlation map of the model is compared with that for the observation in Fig. 4a, we can find the same pattern for the observation, although the values are substantially smaller. There is a negative pole over Greenland and three positive poles at the Far East, western Pacific and southern USA, with the correlations of 0.3, 0.3, and 0.5, respectively. These are statistically significant at the 5% confidence level because the threshold is 0.159 for the degree of freedom 150. The less correlation compared with the model is probably due to the larger transient noise in the observation. From the result, we may suggest that the EOF-1 of the AO mode is a physical mode even for the observed atmosphere.

One point correlation analysis is extended to the target grid points at the other positive center of action in Fig. 1a and 1b at the western Atlantic. The correlation pattern in Fig. 5b for the model is similar to that in Fig. 4b and Fig. 1b. The pattern in Fig. 5a for the observation shows negative pole in high latitudes surrounded by a ring of positive values in mid-latitudes. Since the target grid point in Fig. 5 indicates high correlation with that in Fig. 4, it is reasonable to obtain similar results as Fig. 4. Importantly, the target grid point coincides with one of the wavetrains of the PNA. Therefore, the pattern partly includes the PNA. Although the pattern is deformed by the influence of the PNA, it is considered to represent the AO pattern in Fig. 1 with significant correlation between the Atlantic and Pacific sectors. The result suggests that the AO is a physical mode with dynamical basis. However, we learn from the result that the EOF analysis or one point correlation always involves multiple physical modes.

6. Concluding remarks

Whether the AO is a physical mode or a statistical artifact by the multiple teleconnections of NAO and PNA has been a great concern for the study of understanding the AO. In this respect, the observational fact such that the correlation between Atlantic and Pacific sectors is insignificant (Deser 2000) is the key factor to reject the dynamical theory of explaining the AO.

In this study, similar analysis as Deser (2000) is performed for the barotropic height instead of the sea-level pressure. The essential feature of the low-frequency variability is contained in the barotropic component of the atmosphere which is governed by the 2D fluid mechanics with the inverse energy cascade. The variation in the sea-level pressure is one of the measures of the barotropic dynamics of the global atmosphere, but contains considerable influence by the baroclinic part.

In this study, we first demonstrated that the observed teleconnectivity due to the low-frequency variability is well represented by a simple barotropic model. Since much transient noise is contained in the observation, the model atmosphere can represent the teleconnectivity in pure form. It is confirmed that the teleconnectivity and the PNA is perfectly simulated by the barotropic S-model. The question is focused whether the one point correlation for the NAO is restricted within the Atlantic sector or spread to the Pacific sector surrounding the Arctic.

According to the result, it is found that the one point correlation is not restricted within the Atlantic sector but spread to entire mid-latitudes surrounding the Arctic with a positive poles at the Far East, eastern Pacific, and southern USA. The positive correlations are all statistically significant at the 5% confidence level. The variances explained by the EOF-1 are 5.7% and 15.1% for the observation and model, respectively, when the daily data are analyzed. The contribution increases from 5.7% to 21% when the seasonal (DJF) mean data are analyzed for the observation. It is important to note that the observational data contain large variance in the high-frequency disturbances in short waves, while the model atmosphere contains just the sufficient amount of energy in synoptic waves to support the AO. The short waves, which are not essential for the AO, are damped in the model atmosphere as seen from the energy spectrum in Fig. 2 and Fig. 15 of Tanaka (2003). From this fact, the reduced one point correlation in the observation may be the influence of the transient short-wave noise. The result suggests that the AO is not a statistical artifact due to the multiple teleconnections of the NAO and PNA, but a physical mode with dynamical basis. However, we learn from the experiences that the EOF analysis always involves multiple physical modes, and it is rear to exactly coincide with observation.

Acknowledgments

The study is supported partly by Grant-in-Aids (18204043) of the Japan Society for the Promotion of Science,. Part of the support comes from Asahi Breweries Foundation. The authors appreciate Ms. K. Honda for her technical assistance.

References

Deser, C., 2000: On the teleconnectivity of the Arctic oscillation. *Geophys. Res. Lett.*, **27**, 779–782.

Itoh, H., 2002: True versus apparent Arctic Oscillation. *Geophys. Res. Lett.*, **29**, 1268, doi: 10.1029/ 2001GL013978.

Kalnay, E. M., and Coauthors, 1996: The NCEP/NCAR reanalysis project. *Bull. Amer. Meteor. Soc.*, **77**, 437–471.

Kimoto, M., F.-F. Jin, M. Watanabe, and N. Yasutomi, 2001: Zonal-eddy coupling and a neutral mode theory for the Arctic Oscillation. *Geophys. Res. Lett.*, **28**,737–740.

Tanaka, H. L., 2003: Analysis and modeling the Arctic Oscillation using a simple barotropic model with baroclinic eddy forcing, *J. Atmos. Sci.,* **60**, 1359–1379.

Tanaka, H. L. and M. Matsueda, 2005: Arctic oscillation analyzed as a singular eigenmode of the global atmosphere. *J. Meteor. Soc. Japan*, **83**, 611–619.

Thompson, D. W. J. and J. M. Wallace, 1998: The arctic oscillation signature in the wintertime geopotential height and temperature fields. *Geophys. Res. Lett.*, **25**, 1297–1300.

Wallace, M. and D. S. Gutzler, 1981: Teleconnections in the geopotential height field during the northern hemisphere winter. *Mon. Wea. Rev.*, **109**, 784–812.

Watanabe, M. and F.-F. Jin, 2004: Dynamical prototype of the Arctic Oscillation as revealed by a neutral singular vector. *J. Climate*, **17**, 2119–2138.

Table1. Locations of the center points for the correlation maps

Fig.	Grid point	Fig.	Grid point
4a	(49°N, 170°W)	4b	(49°N, 180°W)
5a	(43°N, 10°W)	5b	(43°N, 10°W)
6a	(37°N, 70°W)	6b	(28°N, 85°W)

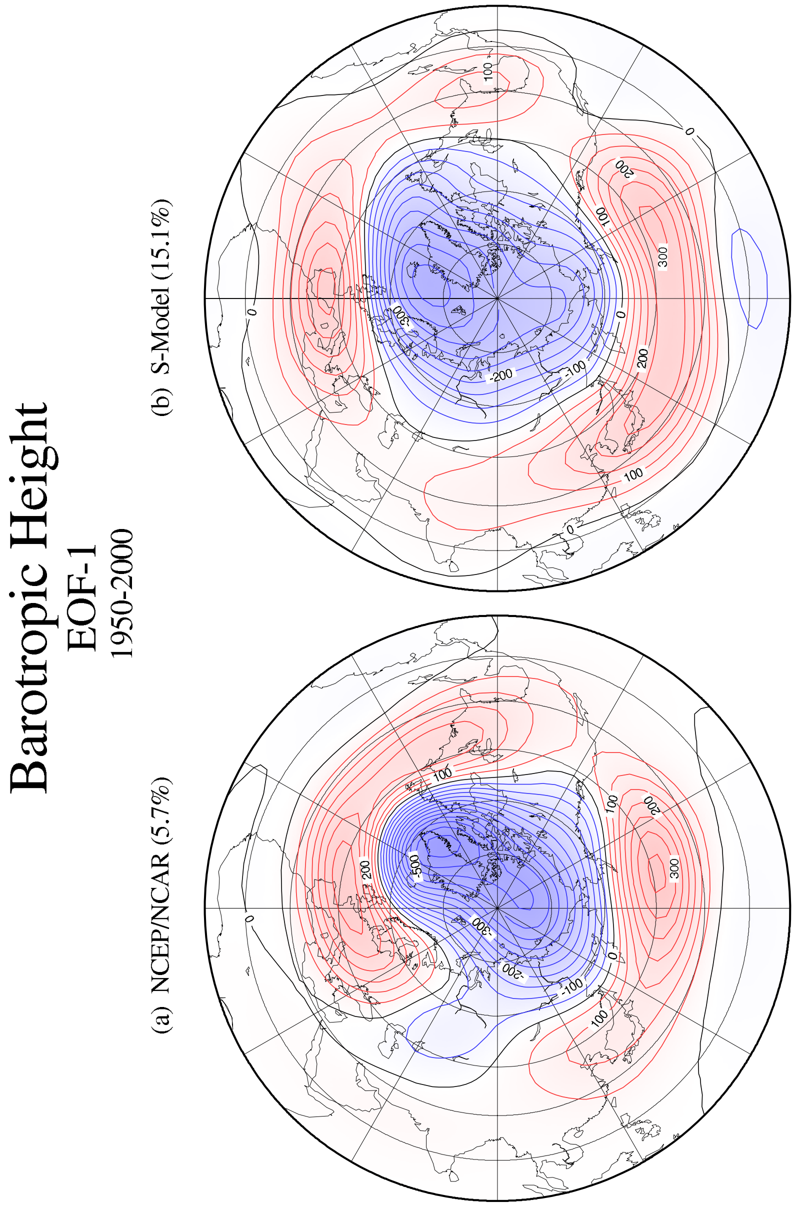

Fig. 1. Barotropic height distribution of the EOF–1 evaluated for DJF of the last 51 years by (a) the NCEP/NCAR reanalysis, (b) the 50-year perpetual January run of the barotropic S-model. The contors are in arbitrary unit.

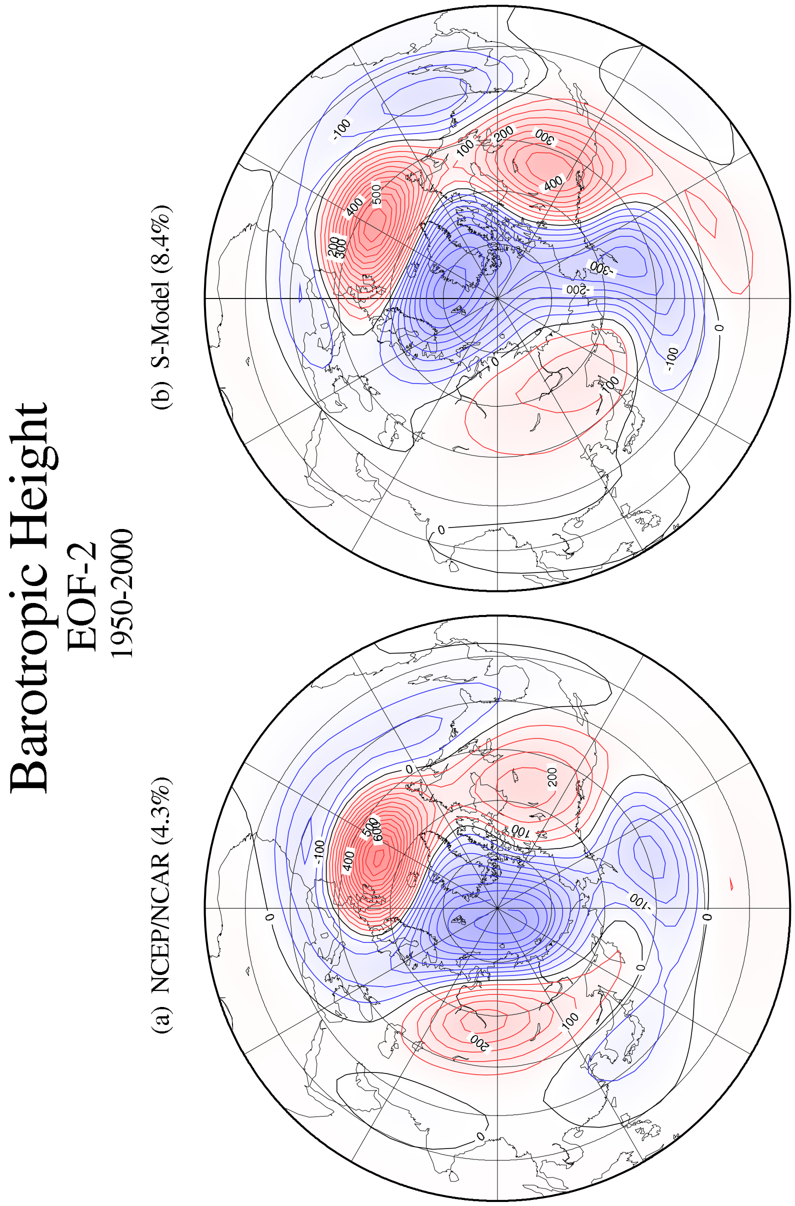

Fig. 2. Barotropic height distribution of the EOF–2 evaluated for DJF of the last 51 years by (a) the NCEP/NCAR reanalysis, (b) the 50-year perpetual January run of the barotropic S-model. The contors are in arbitrary unit.

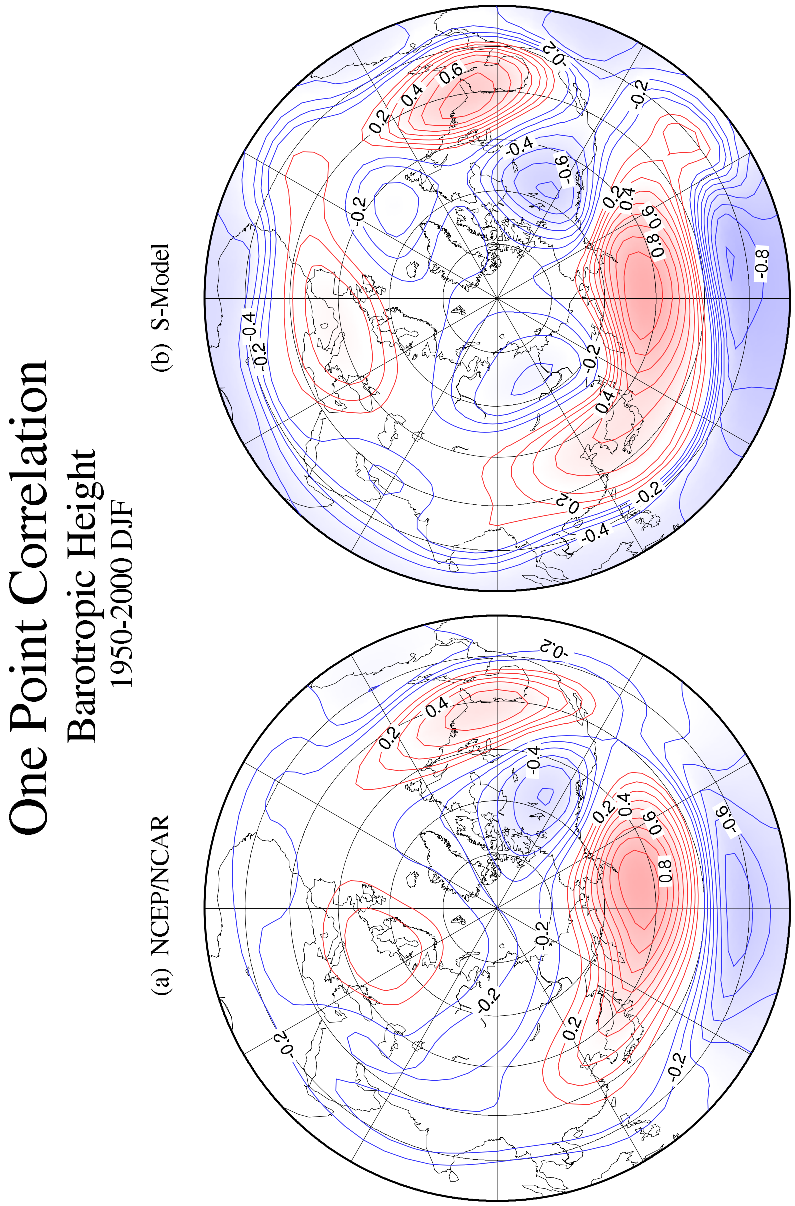

Fig. 3. Distribution of the one point correlation centered at the grid point (a) (49°N, 170°W) for the NCEP/NCAR reanalysis, (b) (49°N, 180°W) for the barotropic S-model.

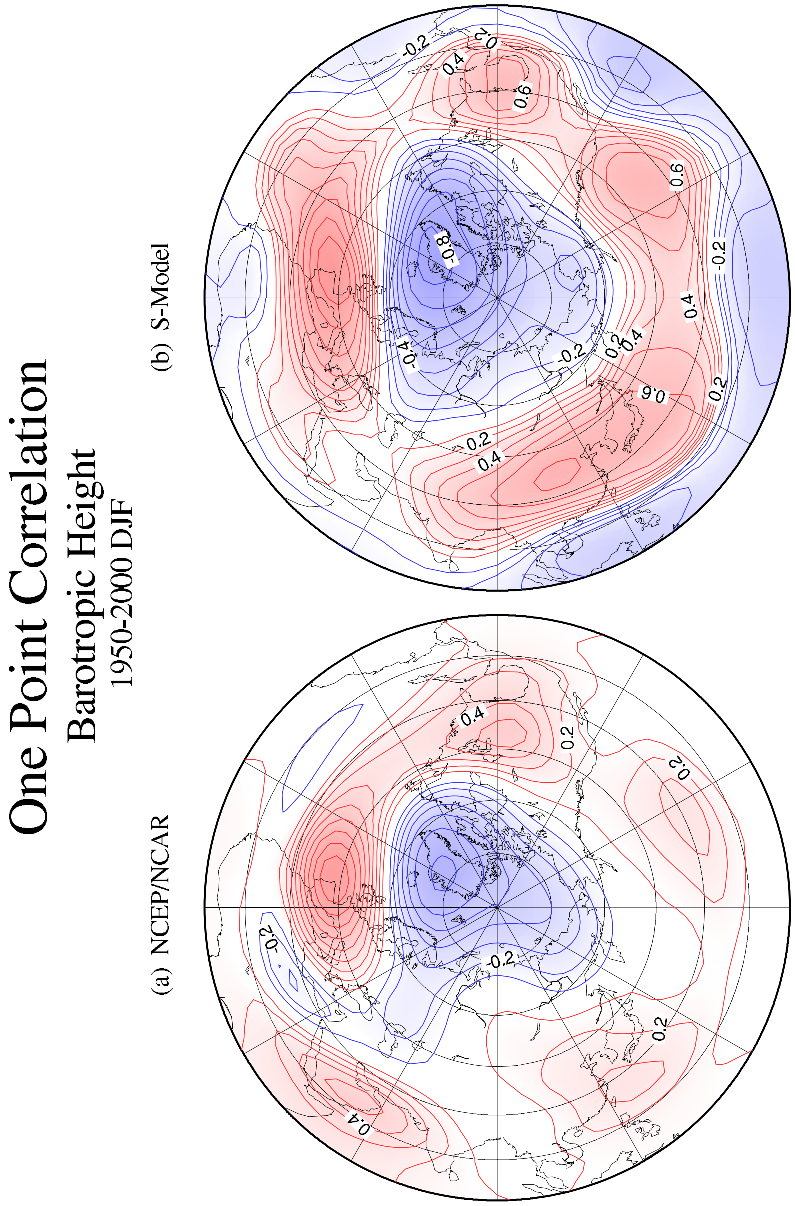

Fig. 4. Distribution of the one point correlation centered at the grid point (a) (43°N, 10°W) for the NCEP/NCAR reanalysis, (b) (43°N, 10°W) for the barotropic S-model.

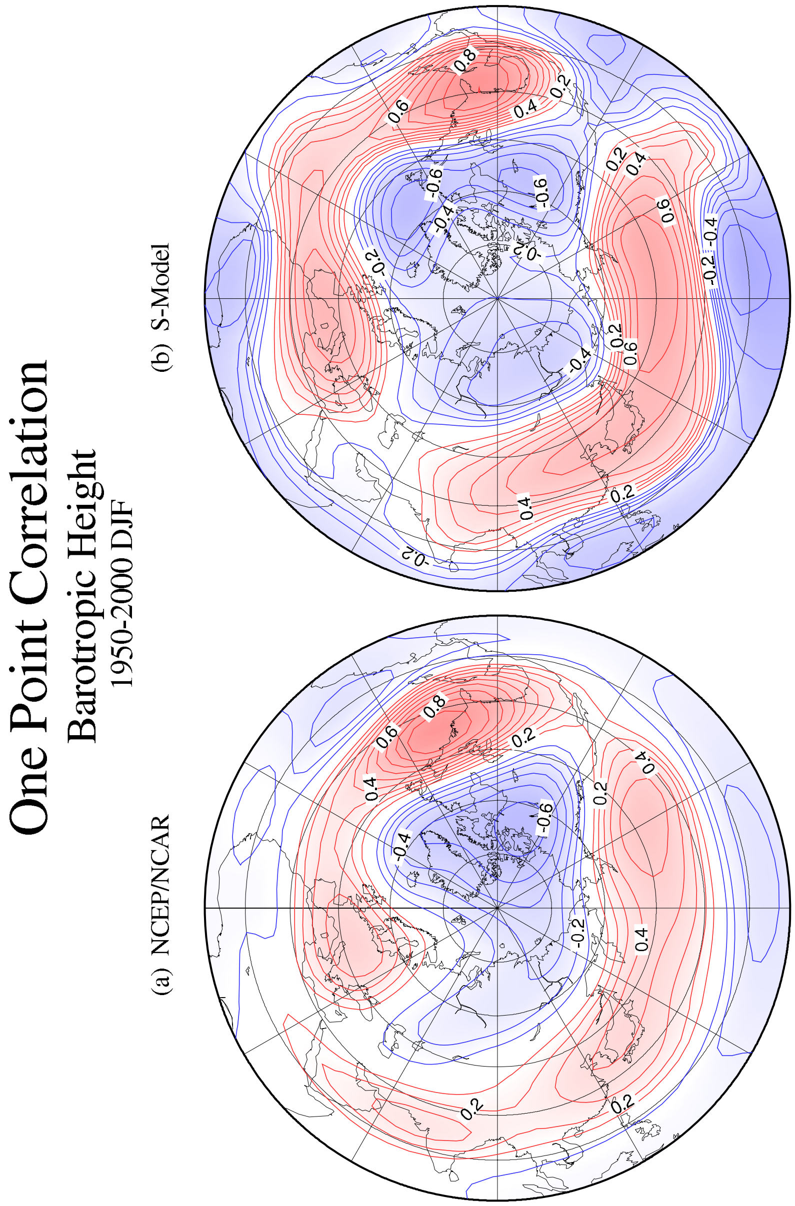

Fig. 5 :Distribution of the one point correlation centered at the grid point (a) (37°N, 70°W) for the NCEP/NCAR reanalysis, (b) (28°N, 85°W) for the barotropic S-model.